Proceedings of the ASME 2024
International Mechanical Engineering Congress and Exposition
IMECE2024
November 17–21, 2024, Portland, OR

IMECE2024-144618

CHANCE CONSTRAINED PDE-CONSTRAINED OPTIMAL DESIGN STRATEGIES UNDER HIGH-DIMENSIONAL UNCERTAINTY

Pratyush Kumar Singh [1], Danial Faghihi[1,*]

[1]University at Buffalo, Buffalo, NY

ABSTRACT

This study focuses on developing a computational framework for model-based design of the thermal insulation elements of net-zero buildings based on silica aerogel porous materials, ensuring they provide superinsulation while upholding structural integrity. This approach employs a multiphase continuum model, capturing the thermomechanical properties of the insulation component through a set of partial differential equations (PDE). The framework considers the uncertainty associated with both the physical parameters like elasticity and thermal conductivity for the solid and fluid phases, as well as the design parameter, which is the spatial distribution of the aerogel porosity over the domain of the component. The combination of spatially varying design and uncertainty parameters, along with their finite element discretization, results in a high dimensional PDE-constrained optimal design problem. A mean cost functional is implemented to achieve both target insulation performance and uncertainty reduction during the design process. To avoid stress concentration in the component, chance constraints are included in the optimization formulation, which ensures that the probability of a function that measures the difference between evaluated stress from the multiphase model and a critical threshold value lies within tolerance. A scalable method is introduced for solving PDE-constrained optimization under uncertainty that is both efficient and dimension-independent. For efficiency, this method exploits a second-order Taylor approximation of the design objective and chance constraint function, which solves a generalized eigenvalue problem. Combined with a gradient-based optimization built on Lagrangian formulation, it results in dimension-independent (scalable) computational costs. The numerical experiments on the design of thermal breaks of the buildings demonstrate that the proposed framework leads to a significant reduction in computational cost while preserving thermal insulation performance and avoiding mechanical failure due to stress concentration.

Keywords: Optimization under uncertainty, Chance constraint, Thermal breaks

*Corresponding author: danialfa@buffalo.edu

1. INTRODUCTION

Thermal breaks play a pivotal role in net-zero buildings by intercepting the path of heat transfer and mitigating the adverse effects of thermal bridging, thereby significantly reducing energy consumption. Silica aerogels, characterized by their lightweight nature and ultra-low thermal conductivity, are poised to revolutionize the next generation of thermal break materials. However, their intrinsic limitation lies in their low mechanical strength, posing a barrier to their widespread adoption in practical applications. Recent advancements in additive manufacturing, particularly the direct ink writing method, offer a promising avenue for addressing this challenge. This method enables the fabrication of components with diverse geometries and spatially varying properties to enhance the aerogel's mechanical properties and expand its functional capabilities. In the context of thermal breaks, high-porosity aerogels exhibit exceptional thermal insulation performance, while low-porosity variants are essential for imparting the necessary mechanical robustness to withstand external loads. Achieving this thermo-mechanical balance necessitates the adoption of simulation-based design methods [1–4], aimed at developing cost-effective components with superior insulation properties and requisite mechanical stability.

This paper presents an efficient computational framework for the optimal design of thermal break components subject to partial differential equation (PDE) constraints and high-dimensional uncertainty, focusing specifically on the spatial distribution of the silica aerogel porosity. The forward PDE model employed herein relies on a two-phase thermo-mechanical model of aerogel based on the continuum theory of mixtures. The design parameter under consideration is the spatial distribution of porosity across the domain, which inherently exhibits spatially correlated uncertainty stemming from material variations and fabrication errors. The optimization objective involves minimizing the mean of the uncertain thermal insulation performance. To ensure the mechanical integrity of the component, chance constraints are imposed on the optimization problem [2, 3], limiting the maximum von

Mises stress induced in the domain to a specified threshold below the critical stress level, thus averting mechanical failure due to excessive stress. To develop a computationally efficient solution algorithm, a second-order Taylor approximation is employed to linearize the optimization cost function and chance constraint. These linearizations leverage the action of the Hessian on a set of random directions, employing a randomized algorithm to solve the associated generalized eigenvalue problem. The optimization procedure is grounded in a gradient-based approach formulated within the Lagrangian framework, ensuring scalability by requiring only a modest number of vectors and their gradients for constructing the design gradient. This results in a framework with computational cost scalability that is independent of the dimensionality of the design parameters. Numerical experiments conducted on thermal breaks for buildings demonstrate that the proposed framework yields a substantial reduction in computational cost compared to Monte Carlo-based estimations of objective function moments and chance constraints.

The structure of the paper is as follows: Section 2 depicts the optimization problem under uncertainty, encompassing the forward model, specification of design and uncertain parameters, and representation of the design objective. Section 3 is devoted to detailing the scalable framework for PDE-constrained chance-constrained optimal design, outlining the Taylor approximation of both the mean cost functional and chance constraint function. In Section 4, the gradient-based optimization method is expounded upon, including the assessment of the cost functional and its gradient concerning design parameters. Section 5 presents the numerical findings regarding optimal design, succeeded by the concluding remarks in Section 6.

2. FORWARD MODEL

The forward model is based on the continuum mixture theory [5]. The model considers two phases which are the incompressible solid aerogel and compressible fluid phases between the materials. The governing equations at steady state for the thermal and mechanical parts can be described using the following PDEs,

$$-\nabla \cdot (\phi_s \kappa_s \nabla \theta_s) = -h(\theta_s - \theta_f) \tag{1}$$

$$-\nabla \cdot (\phi_f \kappa_f \nabla \theta_f) = h(\theta_s - \theta_f) \tag{2}$$

$$Dp = -(\nabla \cdot \boldsymbol{u_s}) \tag{3}$$

$$\nabla . \boldsymbol{T_s'} + (2\phi_f - 1)\nabla p = 0 \tag{4}$$

where model parameters are $\boldsymbol{\theta} = (\kappa_s, \kappa_f, D, \boldsymbol{E_s})$ and states are $\boldsymbol{u} = (\theta_s, \theta_f, \boldsymbol{u_s}, p)$. The state variables $\theta_s, \theta_f, \boldsymbol{u_s}$ and p represent the solid and fluid temperatures, solid displacement, and fluid pressure respectively over the whole domain. The stress tensor is defined as $\boldsymbol{T'} = 2\mu \boldsymbol{E_s} + \lambda\, tr(\boldsymbol{E_s})\boldsymbol{I}$ with $\boldsymbol{E_s} = \frac{1}{2}(\nabla \boldsymbol{u_s} + (\boldsymbol{u_s})^T)$ where $\boldsymbol{E_s}$ is the solid strain and λ and μ are the Lame constants.

Due to the imprecise control of the aerogel ink properties, there is an uncertainty associated with the porosity value within the aerogel thermal break. The uncertain parameter m is represented by a Gaussian measure $\mu = \mathcal{N}(\overline{m}, \mathscr{C})$ with mean $\overline{m}$ and covariance $\mathscr{C}$, which can be represented by a Matern covariance kernel such that $\mathscr{C} = \mathscr{A}^{-2}$ [6]. The design parameter $d(\boldsymbol{x}) \in [0, 1]$ is related to the uncertain and spatially-correlated fluid volume fraction (porosity) $\phi_f(\boldsymbol{x})$, through $\phi_f(\boldsymbol{x}) = g(d(\boldsymbol{x}) + m(\boldsymbol{x}))$, where $g(\cdot)$ is a linear map. Finally, the design objective is defined as thermal compliance of the insulation system as,

$$Q = \frac{1}{2} \sum_{i=s,f} \langle \phi_i \kappa_i \nabla \theta_i, \nabla \theta_i \rangle_\Omega + \sum_{i=s,f} \langle \phi_i h_{air}(\theta_i - \theta_{amb}), \theta_i \rangle. \tag{5}$$

3. SCALABLE FRAMEWORK FOR CHANCE CONSTRAINT OPTIMAL DESIGN

The PDE-constrained optimization under uncertainty problem aims to determine the spatial distribution of porosity within the thermal break, which avoids stress concentration and provides thermal performance. The PDE (1) can be abstractly represented as $\mathscr{R}(u, m, d) = 0$ in $\mathscr{V}'$, where $m \in \mathscr{M}$ denotes an uncertain parameter field residing in a Banach space $\mathscr{M}$ and has a probability distribution μ. To incorporate the uncertainty stemming from the dependence on m into the design process, we use the mean of design objective in the cost functional as,

$$\mathcal{J}(d) = \mathbb{E}[Q(m, d)] + R(d), \tag{6}$$

where the term $R(d)$ represents the regularization term. In this work, we considered Tikhonov regularization, which can be expressed as,

$$R(d) = \int_\Omega \beta_{tik} |\nabla d|^2 \, d\Omega,$$

where β_{tik} is the parameter that controls the interface thickness. To mitigate the risk of stress concentration within the domain, it is imperative that the maximum stress remains below the critical stress threshold. However, due to the non-differentiable nature of the maximum stress, direct optimization poses significant challenges. This can be resolved using stress aggregation function based on p-norm [7], which is a smooth approximation of the maximum stress facilitating the application of gradient-based optimization techniques. For the chance constraint function, we consider the p-norm of the von Mises stress for the component, which approximates its maximum value in the entire domain. The p-norm for the von mises stress can be computed as

$$T_{\text{pn}} = \left(\int_\Omega T_{\text{VM}}^p \, d\Omega \right)^{\frac{1}{p}} \tag{7}$$

The chance constraint function can hence be written as,

$$f = T_{cr} - T_{\text{pn}}, \tag{8}$$

where T_{cr} is the limiting critical stress and T_{pn} is the p-norm of the von Mises stress over the domain. To avoid stress concentration, we consider a chance constraint:

$$P(f(m, d) \geq 0) \leq \alpha_c, \tag{9}$$

for a critical chance $0 < \alpha_c < 1$. The probability is given by

$$\begin{aligned} P(f(m, d) \geq 0) &= \mathbb{E}[\mathbb{I}_{[0,\infty]}(f(m, d))] \\ &= \int_{\mathscr{M}} \mathbb{I}_{[0,\infty]}(f(m, d)) \, d\mu(m), \end{aligned} \tag{10}$$

where $\mathbb{I}_{[0,\infty]}(f(m,d))$ is an indicator function defined as:

$$\mathbb{I}_{[0,\infty]}(f(m,d)) = \begin{cases} 1 & \text{if } f(m,d) \geq 0 \\ 0 & \text{if } f(m,d) < 0 \end{cases}$$

Hence, the PDE-constrained optimization can be written as,

$$\min_d \mathcal{J}(d) \text{ subject to (1)-(4) and chance constraint (9).} \quad (11)$$

3.1 Taylor Approximation

Due to the requirement of large PDE evaluations in the sample averaged calculation of the mean in the cost functional, Taylor approximation is applied for both the objective function and the constraint function, which requires an efficient eigenvalue decomposition of the Hessian of the objective and constraint functions with respect to the random parameter field. We assume that the objective function Q can be approximated as a second-order Taylor expansion centered around the mean of the uncertain parameter $\overline{m}$, which is given by

$$T_2Q(m,d) = \sum_{k=0}^{2} \partial_m^k Q(\overline{m},d)(m-\overline{m})^k \quad (12)$$

The closed form for the expectation of the quadratic Taylor approximation $\mathcal{J}_{quad}$ is defined as:

$$\mathcal{J}_{quad} = \mathbb{E}[T_2Q(d)] = Q(\overline{m},d) + \frac{1}{2}tr(\overline{\mathcal{H}}_q) \quad (13)$$

where $tr(\overline{\mathcal{H}}_q)$ represents the trace of $\mathcal{H}_q$ which is the covariance-preconditioned Hessian of the objective Hessian Q. The eigenvalues λ_n are obtained by solving the following generalized eigenvalue problem,

$$\langle \zeta, \nabla^2_{mm} Q\, \psi_j \rangle = \lambda_j \langle \zeta, \mathcal{C}^{-1}\psi_j \rangle,\ \forall \zeta \in \mathcal{M},\ j = 1, ..., N_{eig} \quad (14)$$

where the eigenvectors ψ_j exhibit orthonormality with $\mathcal{C}^{-1}, \langle \psi_i, \mathcal{C}^{-1}\psi_j \rangle = \delta_{ij}, i, j = 1, ...N_{eig}$ and δ_{ij} denote the Kronecker delta function. Using an n-degree finite element discretization, 14 can be written as $\boldsymbol{A\psi} = \lambda \boldsymbol{B\psi}$. The eigenvalue problem at hand can be effectively solved using a double-pass randomized algorithm [8]. Subsequently, the obtained eigen-decomposition is employed to estimate the trace of the covariance-preconditioned Hessian $\mathcal{H}_q$ via its dominant eigenvalues λ, expressed as,

$$tr(\overline{\mathcal{H}_q}) = \sum_{n=1}^{N_q} \lambda_n, \quad (15)$$

where, N_q represents the low-dimensional dominant modes. As demonstrated in the results section, N_q is invariant to the parameter dimension, and the eigenvalues exhibit rapid decay for numerous problems when the covariance-preconditioned Hessian is low-rank.

We construct a second-order Taylor expansion of the constraint function f at $\overline{m}$ similar to (13) denoted by $T_2 f$ to facilitate approximation of the probability $P(f(m,z) \geq 0)$ through sampled averaged approximation as:

$$P(f(m,d)) \geq 0) \approx f_M^2(d) = \frac{1}{M_f}\mathbb{I}_{[0,\infty)}(T_2 f(m_i,d)). \quad (16)$$

This approximation of the constraint function obviates the necessity for a large number of PDE solves to assess the probability utilizing sample averaging methods.

4. GRADIENT-BASED OPTIMIZATION

A gradient-based approach is employed to tackle the chance-constrained optimization problem outlined in the preceding section. Specifically, the Newton Conjugate Gradient algorithm is employed, which constitutes a modified variant of Newton's method. This algorithm leverages the conjugate gradient technique to compute the inverse of the local Hessian matrix. The optimization process necessitates the incorporation of four key components: (1) a smooth approximation of the indicator function, (2) a penalty method for handling inequality chance constraints, (3) a continuation scheme to refine both the smooth approximation and the penalty term associated with inequality chance constraints, and (4) the calculation of the gradient of the quadratic approximate cost functional $\mathcal{J}_{quad}$. This section elaborates the entire methodology to solve the optimization problem.

4.1 Smooth approximation

The indicator function utilized in the chance constraint exhibits discontinuity at $f(m,d) = 0$. In order to employ a gradient-based optimization method, this discontinuous indicator function must be approximated with a smooth, continuous counterpart. One approach involves employing a logistic function as a smooth approximation of the indicator function such that,

$$\mathbb{I}_{[0,\infty]}(x) \approx l_\beta(x) = \frac{1}{1+e^{-2\beta x}}, \quad (17)$$

where a larger β corresponds to a sharper transition at $x = 0$.

4.2 Penalty Method

To impose the inequality constraint (9), a quadratic penalty method [9] is applied. The quadratic penalty function is defined as,

$$S_\gamma(x) = \frac{\gamma}{2}(max\{0,x\})^2 \quad (18)$$

where $\gamma > 0$ is a constant corresponding to the weight of the penalty. Using the penalty method, the chance-constrained problem can be rewritten as

$$\min_{d\in[0,1]} \mathcal{J}(d) + \mathcal{S}_\gamma(\mathbb{E}[l_\beta(f)] - \alpha_c) \quad (19)$$

Let $\mathcal{J}(d)$ denote the approximation of the cost functional in (6), and $\nabla_d \mathcal{J}$ denote the gradient of cost functional with respect to design variable. A continuation scheme [3] is utilized, which gradually increases the smoothing parameter β and penalty parameter γ inside an outer loop and Newton Conjugate Gradient optimizer.

4.3 Adaptive optimization

The gradient-based scheme uses a continuation scheme that gradually increases the smoothing parameter β and penalty parameter γ to achieve convergence [3]. An initial value of the smoothing parameter β_0 and the penalty parameter γ_0 is defined for the continuation scheme. These parameters are updated at the end of each iteration using scaling parameters σ_β and σ_γ for smoothing and penalty parameters, respectively. For k^{th} iteration , the updated smoothing parameter is $\beta_{k+1} = \sigma_\beta \beta_k$ and the updated penalty parameter is $\gamma_{k+1} = \sigma_\gamma \gamma_k$. In an outer loop, we update the parameters β and γ, whereas a Newton Conjugate Gradient (Newton CG) is applied in the inner loop to solve the optimization problem (19). The stopping criterion for the outer loop is if the maximum number of iterations $k_{\max}$ is reached. For each iteration, the approximated chance is computed through the quadratic approximation f_M^2 of the chance function as given in (16). The output is the optimal value of design parameter d_{opt}. The algorithm for this adaptive optimization is given in Algorithm 1.

Algorithm 1

Input: $d_0, \beta_0, \gamma_0, \sigma_\beta, \sigma_\gamma, \hat{f} = f_M^2(d)$

while $||d_k - d_{k-1}|| \leq \epsilon_{\text{out}}$ or $k < k_{\max}$

1. d_{k+1} = Newton CG$(d_k, \mathcal{J}(d), \nabla_d \mathcal{J}(d), \epsilon_{\text{in}})$.
2. Evaluate approximate chance $\hat{f}_{k+1}$ at d_{k+1}.
3. Update $\beta_{k+1} = \sigma_\beta \beta_k$, $\gamma_{k+1} = \sigma_\gamma \gamma_k$

end while

return d_{opt}

4.4 Computation of gradient of cost functional

The gradient and Hessian of design objective Q with respect to uncertain parameter m are known as m_Q-gradient and m_Q-Hessian; also, the gradient and Hessian of constraint function f with respect to m are known as m_f-gradient and m_f-Hessian. An approximate cost functional using Taylor approximation and its gradient with respect to the design variable is computed using a gradient-based algorithm. Lagrangian formulation is employed to derive the gradient of the quadratic approximation of the design objective $\mathcal{J}_{quad}$ with respect to the design parameter d denoted as d-gradient. A Lagrangian functional is created by enforcing all the PDE constraints. Setting the variation of Lagrangian as zero with respect to state variables, adjoint variables, and eigenvalues, we can come up with a set of incremental state problems, incremental adjoint problems, linear state problems, and linear adjoint problems. The algorithm for computing the d-gradient is given in Algorithm 2.

Algorithm 2

1. Solve for m_Q-gradient and m_Q-Hessian
2. Solve for m_f-gradient and m_f-Hessian.
3. Solve for generalized eigenpairs with double-pass randomized algorithm.
4. Compute approximate cost functional $\mathcal{J}_{quad}$ by (13)
5. Solve the linear state problem.
6. Solve the linear adjoint problem.
7. Obtain the d-gradient.

---

5. RESULTS AND DISCUSSIONS

This section presents numerical experiments conducted on an insulation component with the objective of maximizing thermal insulation performance while ensuring adequate mechanical stability through the incorporation of chance constraints. The numerical results aim to assess the impact of critical chance, limiting critical stress value, Tikhonov regularization weight, smoothing, and penalty parameters. The problem under consideration entails an L-shaped geometry. For the heat transfer model, Neumann boundary conditions are imposed, with ambient temperatures set at 1 and 0 at the outer and inner boundaries, respectively, and insulated conditions applied to the remaining two boundaries. The boundary conditions of the mechanical model involve prescribing a uniform traction load with magnitude 1 along and in the opposite direction of the unit vectors on the outer boundary, fixing solid displacement on the inner boundary, and applying roller conditions to the other boundaries. Model parameters are specified as $\kappa_s = 0.477$, $\kappa_s = 0.085$, $h = 81059$, $C = 0.25$, $\lambda = 6.77$, and $\mu = 3.38$, adopted from the previous research [5]. The uncertain parameter m is the Gaussian random field with Matern covariance and mean $\overline{m} = 0$ and correlation length $L_C = 0.02$. Figure 1 shows some samples of the uncertain parameter used in the numerical experiments.

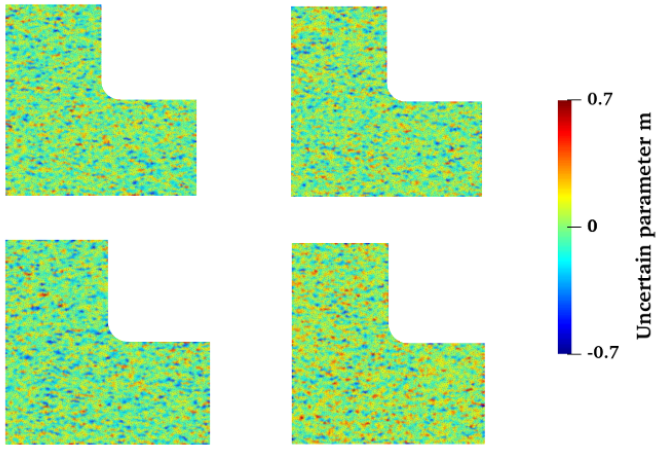

FIGURE 1: Samples of uncertain parameter m with correlation length $L_C = 0.02$

In all numerical examples, a finite element mesh with 8587 nodes is utilized. The proposed design under uncertainty framework is implemented leveraging a suite of open-source libraries, including FEniCS [10] for finite element solution of the forward model, hIPPYLib [11–13] for the trace estimator and Newton conjugate gradient algorithm, and SOUPy [14] for quadratic approximation of the design objective.

5.1 Scalability of the optimization algorithm

Figure 4 depicts the decay of eigenvalues in (14) for various dimensions of design and uncertain parameters, denoting different finite element discretizations. The consistent nature of the eigenvalue decay across these dimensions underscores the scalability of the quadratic approximation with respect to the parameter dimension. In other words, the computational cost of the proposed

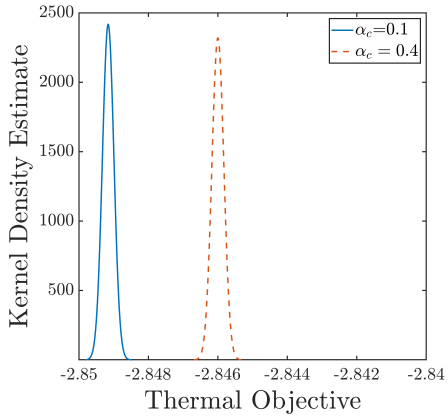

FIGURE 2: The probability distribution of the thermal objective Q for the designed components at different values of α_c

design under an uncertainty framework is independent of the number of designs and uncertain parameters but rather depends on the low rank of the preconditioned Hessian.

5.2 Effect of critical chance

The critical chance α_c represents the probability threshold beyond which the p-norm of von Mises stress may exceed the limiting critical stress. Therefore, α_c signifies the accepted degree of uncertainty in stress concentration to prevent mechanical failure of the insulation component. Figure 3 illustrates the optimal design results achieved by setting α_c to two distinct values. The limiting critical stress T_{cr} for both cases is 1.6 MPa. Additionally, this figure presents the corresponding states, and von Mises stress assessed at the mean of the uncertain parameters. The findings suggest that considering a higher critical chance entails the placement of mechanically stronger material (shown in red) over a broader region of the domain, resulting in diminished local stress values across the component. However, enhancing stability with higher α_c values will come at the expense of the insulation performance of the component, as evidenced by the probability distribution of thermal compliance depicted in Figure 2.

5.3 Effect of Tikhonov weight

Next, we explore the impact of Tikhonov regularization by considering two different weights: $\beta_{tik} = 1 \times 10^{-4}$ and $\beta_{tik} = 2 \times 10^{-4}$, depicted in Figure 5. As illustrated in this figure, stronger regularization yields smoother optimal design solutions within the domain, resulting in increased interface thickness between the two materials. For more intricate problems, it may be necessary to enhance regularization to achieve a nearly sharp interface [4].

5.4 Effect of smoothing and penalty parameter

We demonstrate the effect of the scaling parameters σ_β and σ_γ. The effect of scaling parameter σ_β is demonstrated in two cases. As the smoothing parameter β increases, the approximation to the indicator function becomes more accurate, and hence the solution starts to improve. Figure 6 shows the convergence of the value of chance $l_\beta f$ for two different values of scaling parameter σ_β while keeping the other parameters constant. The

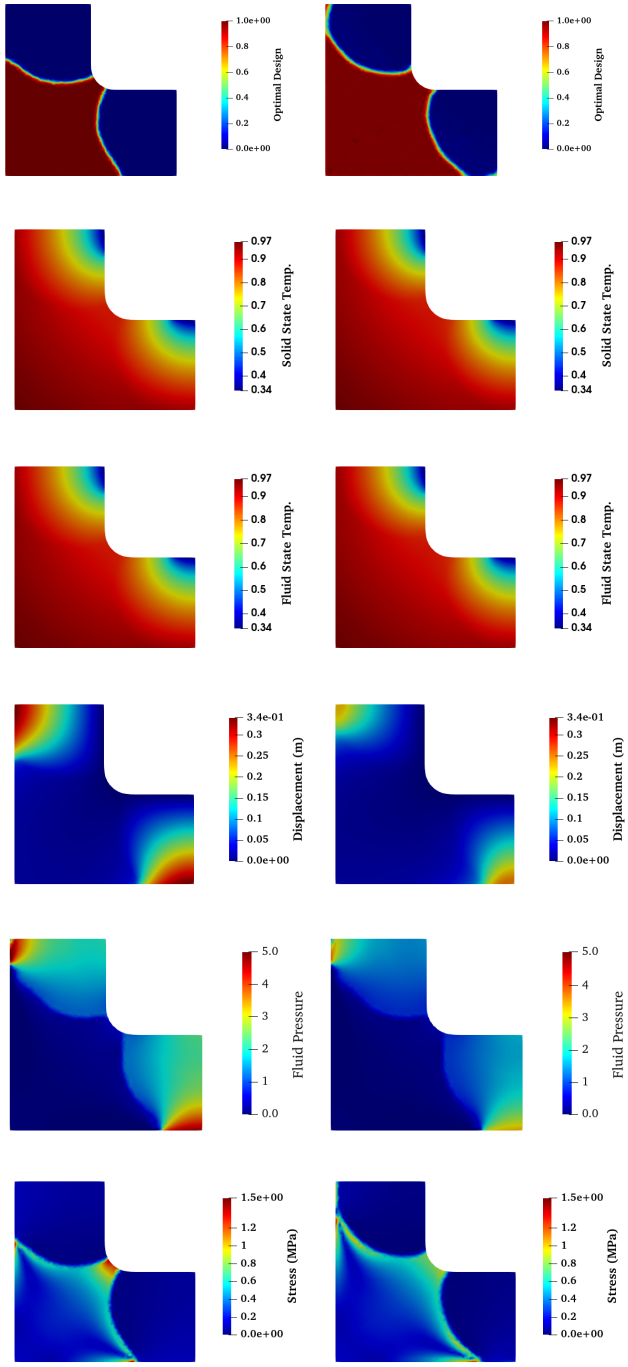

FIGURE 3: Effect of the critical chance parameter α_c on the optimal design of the insulation component: (a) α_c = 0.1 and (b) α_c = 0.4. Each row displays the optimal design corresponding to different material porosity settings, along with the corresponding states (solid and fluid temperatures, solid displacement, and fluid pressure) and von Mises stress, all evaluated at the mean of the uncertain parameters $\overline{m}$.

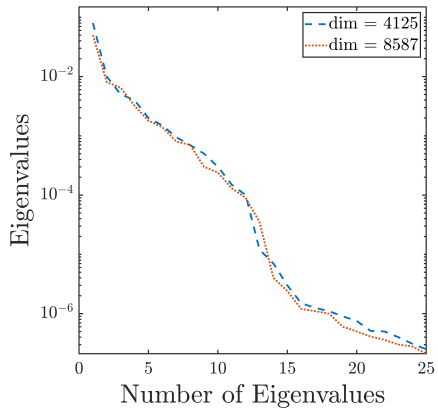

FIGURE 4: Decay of the eigenvalues for the quadratic approximation with different uncertain parameter dimensions (mesh discretizations) indicating that the quadratic approximation results in a scalable design under uncertainty algorithm.

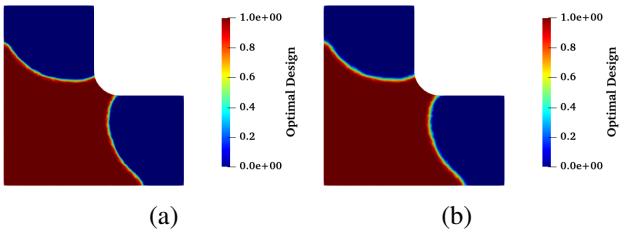

FIGURE 5: Effect of Tikhonov weight on the optimal design solutions: (a) $\beta_{\text{tik}} = 1 \times 10^{-4}$ and (b) $\beta_{\text{tik}} = 2 \times 10^{-4}$

convergence of $l_\beta f$ is observed with an increasing number of iterations k in Algorithm 1. When the value of σ_β is higher, the value of computed chance l_β is much closer to the value of critical chance $\alpha_c = 0.1$. As the scaling factor for penalty parameter σ_γ increases, the violation of critical chance α_c is strongly penalized, and it leads to a reduction in the number of function calls required to attain convergence. Here, the number of functional calls refers to the number of times the function inside the Newton CG algorithm is evaluated for computing the gradient and the hessian. The number of function calls is related to the computational cost. If the number of function calls is high, then the computational cost is also high, and vice-versa. We analyze the effect of scaling parameter σ_γ on the number of function calls for the optimization problem (19). Figure 7 shows the reduction in the number of functional calls with an increasing number of iteration k as we closely move towards the optimal solution d_{opt}, as explained for Algorithm 1. As illustrated in Figure 7, the number of function calls required for $\sigma_\gamma = 1000$ is less as compared to $\sigma_\gamma = 100$. This shows that stronger penalization leads to faster convergence for obtaining the optimal solution d_{opt}, with less number of function calls.

6. CONCLUSIONS

This paper presents an efficient and scalable computational framework for chance-constrained optimal design under high-dimensional uncertainty for systems governed by PDEs. To capture spatially correlated uncertainty, a Gaussian random field with a Matern covariance kernel is utilized, requiring the solution of a stochastic PDE. To address challenges posed by high-dimensional parameter spaces, an approximation method is proposed to solve the resultant optimization problem, ensuring computational cost remains invariant to the number of design parameters. To handle discontinuous indicator functions and inequality constraints, a smooth approximation and a penalty method within a continuation Newton conjugate gradient algorithm are taken into account.

The framework is applied to the design of thermal insulation components in building envelopes utilizing silica aerogel porous materials. The material behavior is governed by a thermo-mechanical model of aerogel based on the continuum theory of mixtures. The design parameter of interest is the spatial distribution of porosity across the domain, inherently exhibiting uncertainty due to material variations and fabrication errors. The cost functional comprises the mean of thermal insulation properties, with chance constraints imposed on the optimization problem to limit the maximum von Mises stress in the domain below a specified threshold, to prevent mechanical failure due to excessive stress. Application of the proposed framework to

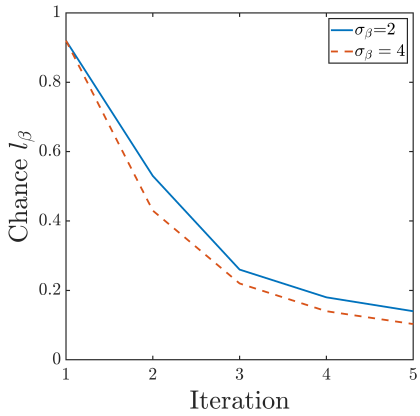

FIGURE 6: Effect of parameter σ_β on the convergence of the value of chance.

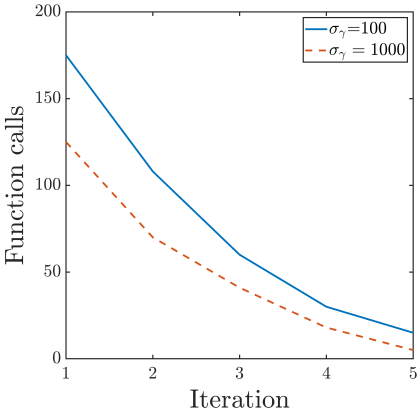

FIGURE 7: Effect of parameter σ_γ on the reduction in the number of functional calls with an increasing number of iteration.

the design of building insulation components aims to achieve both thermal insulation and mechanical stability. The impact of critical chance, limiting critical stress value, Tikhonov regularization weight, smoothing, and penalty parameters on the designed spatial distribution of material porosity and corresponding thermal and mechanical performances is investigated. The results highlight the efficacy of the proposed design under uncertainty framework, offering orders of magnitude reduction in computational cost compared to sampling-based methods for handling the design objective moments and constraints. In future work, the proposed method will be expanded to account for uncertainty in material model parameters, characterized via Bayesian model calibration, e.g., [5, 15–18] using experimental measurements of thermal and mechanical properties of silica aerogel, e.g., [19].

REFERENCES

[1] Chen, Peng, Quarteroni, Alfio and Rozza, Gianluigi. "A weighted reduced basis method for elliptic partial differential equations with random input data." *SIAM Journal on Numerical Analysis* Vol. 51 No. 6 (2013): pp. 3163–3185.

[2] Chen, Peng, Villa, Umberto and Ghattas, Omar. "Taylor approximation and variance reduction for PDE-constrained optimal control under uncertainty." *Journal of Computational Physics* Vol. 385 (2019): pp. 163–186.

[3] Chen, Peng and Ghattas, Omar. "Taylor approximation for chance constrained optimization problems governed by partial differential equations with high-dimensional random parameters." *SIAM/ASA Journal on Uncertainty Quantification* Vol. 9 No. 4 (2021): pp. 1381–1410.

[4] Tan, Jingye and Faghihi, Danial. "A scalable framework for multi-objective PDE-constrained design of building insulation under uncertainty." *Computer Methods in Applied Mechanics and Engineering* Vol. 419 (2024): p. 116628.

[5] Tan, Jingye, Maleki, Pedram, An, Lu, Di Luigi, Massimigliano, Villa, Umberto, Zhou, Chi, Ren, Shenqiang and Faghihi, Danial. "A predictive multiphase model of silica aerogels for building envelope insulations." *Computational Mechanics* Vol. 69 No. 6 (2022): pp. 1457–1479.

[6] Lindgren, Finn, Rue, Håvard and Lindström, Johan. "An explicit link between Gaussian fields and Gaussian Markov random fields: the stochastic partial differential equation approach." *Journal of the Royal Statistical Society Series B: Statistical Methodology* Vol. 73 No. 4 (2011): pp. 423–498.

[7] Le, Chau, Norato, Julian, Bruns, Tyler, Ha, Christopher and Tortorelli, Daniel. "Stress-based topology optimization for continua." *Structural and Multidisciplinary Optimization* Vol. 41 (2010): pp. 605–620.

[8] Saibaba, Arvind K., Lee, Jonghyun and Kitanidis, Peter K. "Randomized algorithms for generalized Hermitian eigenvalue problems with application to computing Karhunen–Loève expansion." *Numerical Linear Algebra with Applications* Vol. 23 No. 2 (2016): pp. 314–339.

[9] Nocedal, Jorge and Wright, Stephen J. "Quadratic programming." *Numerical optimization* (2006): pp. 448–492.

[10] Alnæs, Martin S., Blechta, Jan, Hake, Johan, Johansson, August, Kehlet, Benjamin, Logg, Anders, Richardson, Chris, Ring, Johannes, Rognes, Marie E. and Wells, Garth N. "The FEniCS Project Version 1.5." *Archive of Numerical Software* Vol. 3 No. 100 (2015). DOI 10.11588/ans.2015.100.20553.

[11] Villa, U., Petra, N. and Ghattas, O. "hIPPYlib: an Extensible Software Framework for Large-scale Deterministic and Bayesian Inverse Problems." (2016)DOI 10.5281/zenodo.596931. URL http://hippylib.github.io.

[12] Villa, U., Petra, N. and Ghattas, O. "hIPPYlib: an Extensible Software Framework for Large-scale Deterministic and Bayesian Inverse Problems." *Journal of Open Source Software* Vol. 3 No. 30 (2018). DOI 10.21105/joss.00940.

[13] Villa, Umberto, Petra, Noemi and Ghattas, Omar. "HIPPYlib: An Extensible Software Framework for Large-Scale Inverse Problems Governed by PDEs: Part I: Deterministic Inversion and Linearized Bayesian Inference." *ACM Trans. Math. Softw.* Vol. 47 No. 2 (2021). DOI 10.1145/3428447. URL https://doi.org/10.1145/3428447.

[14] Chen, Peng. "Stochastic Optimization under high-dimensional Uncertainty in Python." https://github.com/cpempire/soupy.git (2022).

[15] Liang, Baoshan, Tan, Jingye, Lozenski, Luke, Hormuth, David A, Yankeelov, Thomas E, Villa, Umberto and Faghihi, Danial. "Bayesian inference of tissue heterogeneity for individualized prediction of glioma growth." *IEEE Transactions on Medical Imaging* Vol. 42 No. 10 (2023): pp. 2865–2875.

[16] Tan, Jingye, Liang, Baoshan, Singh, Pratyush Kumar, Farrell-Maupin, Kathryn A and Faghihi, Danial. "Toward selecting optimal predictive multiscale models." *Computer Methods in Applied Mechanics and Engineering* Vol. 402 (2022): p. 115517.

[17] Lima, Ernesto ABF, Faghihi, Danial, Philley, Russell, Yang, Jianchen, Virostko, John, Phillips, Caleb M and Yankeelov, Thomas E. "Bayesian calibration of a stochastic, multiscale agent-based model for predicting in vitro tumor growth." *PLoS Computational Biology* Vol. 17 No. 11 (2021): p. e1008845.

[18] Tan, Jingye, Villa, Umberto, Shamsaei, Nima, Shao, Shuai, Zbib, Hussein M and Faghihi, Danial. "A predictive discrete-continuum multiscale model of plasticity with quantified uncertainty." *International Journal of Plasticity* Vol. 138 (2021): p. 102935.

[19] An, Lu, Liang, Baoshan, Guo, Zipeng, Wang, Jieyu, Li, Changning, Huang, Yulong, Hu, Yong, Li, Zheng, Armstrong, Jason N, Zhou, Chi et al. "Wearable aramid–ceramic aerogel composite for harsh environment." *Advanced Engineering Materials* Vol. 23 No. 3 (2021): p. 2001169.